

How to Cite:

Magar, S. D., & Pawar, P. Y. (2022). In silico ADMET screening & molecular docking of some 1-(5-(4-chlorophenyl)-1,3,4-oxadiazol-3(2H)-yl) ethanone derivatives to be developed as triple mutant T790M/C797S EGFR inhibitors. *International Journal of Health Sciences*, 6(S3), 10432–10451. <https://doi.org/10.53730/ijhs.v6nS3.9448>

In silico ADMET screening & molecular docking of some 1-(5-(4-chlorophenyl)-1,3,4-oxadiazol-3(2H)-yl) ethanone derivatives to be developed as triple mutant T790M/C797S EGFR inhibitors

Sagar D. Magar

Department of Pharmaceutical Chemistry, Dr. Vitthalrao Vikhe Patil Foundation's, College of Pharmacy, Ahmednagar, Maharashtra, 414111, India

*Corresponding author email: sagarmagar2010@gmail.com

Orcid ID: <https://orcid.org/0000-0001-8467-849X>

Dr. Pratap Y. Pawar

Department of Pharmaceutical Chemistry, Dr. Vitthalrao Vikhe Patil Foundation's, College of Pharmacy, Ahmednagar, Maharashtra, 414111, India

Abstract--- EGFRs' high expression and/or adaptive activation coincides with the pathogenesis and development of many tumors, making them appealing candidates for both diagnosis and therapy. Several strategies for targeting these receptors and/or the EGFR-mediated effects in cancer cells have been established. A lot of in silico models are developed for prediction of chemical ADMET properties. However, it is still not easy to evaluate the drug-likeness of compounds in terms of so many ADMET properties. In present study, we have designed some 1-(5-(4-chlorophenyl)-1, 3, 4-oxadiazol-3(2H)-yl) ethanone derivatives to be developed as potential EGFR inhibitors for the treatment of cancer. The designed derivatives were screened through Lipinski rule, Veber's rule, ADMET analysis, drug-likeness properties and molecular docking. We concluded that all the compounds sm1, sm2, sm3, sm8, sm9, sm10, sm11, sm12, sm13, sm14, sm15, sm18, and sm19 were found to possess drug-likeness properties and therefore were subjected for molecular docking studies. From molecular docking studies it was observed that Molecules Sm3, Sm8, Sm9, Sm10, Sm12, and Sm2 had formed either three or two conventional hydrogen bonds with EGFR enzyme and hence selected for synthesis which can be developed further to get more promising molecules for the treatment of cancer.

Keywords---EGFR, angiogenesis, cancer, ADMET, molecular docking.

Introduction

Radiation and chemotherapy are effective against a wide variety of malignancies, but molecular targeting medicines for cancer treatment can target specific types of tumours with greater accuracy. Progress has been achieved over the last few decades in uncovering the complex cellular, metabolic and genetic processes that lead to cancer formation and progression(1). More tumor-targeted anticancer treatments have been developed because to this improved understanding of how cancer works. Tumor development and proliferation have been linked to tyrosine kinases, which are frequent therapeutic targets. By blocking downstream signalling pathways from activating, tyrosine kinase inhibitors (TKIs) prevent the related kinases from phosphorylating their substrates' tyrosine residues(2). Over the last two decades, a number of robust and well-tolerated TKIs targeting single or multiple targets, such as EGFR, ALK, ROS1, HER2, NTRK, VEGFR, RET, MET, MEK, FGFR, PDGFR, and KIT, have been developed, advancing our understanding of precision cancer medicine based on a patient's genetic alteration profile(3). The epidermal growth factor receptor (EGFR) has been identified as a molecular target for certain potential cancer therapies. Four transmembrane tyrosine kinases (EGFR1/ErbB1, Her2/ErbB2, Her3/ErbB3, and Her4/ErbB4), as well as thirteen secreted polypeptide ligands, make up the EGFR family(4). Multiple solid tumours, including breast, pancreatic, head and neck, kidney, vaginal, renal, colon, and non-small-cell lung cancer, have overexpressed EGFRs(5). Overexpression of these genes causes cell proliferation, differentiation, cell cycle progression, angiogenesis, cell motility, and apoptosis inhibition through stimulating downstream signaling channels(6). We will be able to quantify the individual activities of EGFR signalling networks as our understanding of their involvement in tumour activity advances. The high expression and/or adaptive activation of EGFRs correlates with the pathophysiology and progression of many cancers, making them attractive candidates for diagnostics and treatment. Several techniques have been developed to target these receptors and/or the EGFR-mediated effects in cancer cells. Monoclonal antibodies (mAbs) that specifically target the EGFR extracellular domain, such as cetuximab (Erbix), and small molecule TKIs that particularly target the EGFR catalytic domain, such as gefitinib (Iressa) and erlotinib(Tarceva), are two types of EGFRIs(7–11).

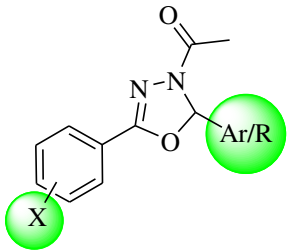
A lot of *in silico* models are hence developed for prediction of chemical ADMET properties. However, it is still not easy to evaluate the drug-likeness of compounds in terms of so many ADMET properties(21–28). In the present work we have performed *in silico* ADMET screening of designed derivatives to be developed as potential EGFR inhibitors for the treatment of cancer. All the designed derivatives were subjected for the calculations of different ADMET parameters to select most promising compound which can possess more drug-likeness properties.

Material and Methods

Designing of 1-(5-(4-chlorophenyl)-1, 3, 4-oxadiazol-3(2H)-yl)ethanone derivatives

The reaction was achieved by heating the aldehydes with 4-chlorobenzohydrazide in the presence of ethanol & sulfuric acid to form 4-chloro-N'-methylenebenzohydrazide. Further 4-chloro-N'-methylenebenzohydrazide undergoes internal cyclization when refluxed to give fused 1-(5-(4-chlorophenyl)-1, 3, 4-oxadiazol-3(2H)-yl) ethanone derivatives. This reaction will be carried out in presence of acetic anhydride. The structure of the parent compound and the substituted azole derivatives are depicted in Table 1.

Table 1
1-(5-(4-chlorophenyl)-1, 3, 4-oxadiazol-3(2H)-yl) ethanone derivatives

 <p>1-(5-(4-chlorophenyl)-1,3,4-oxadiazol-3(2H)-yl) ethanone derivatives</p>			
Code	R/Ar	Code	R/Ar
sm1	H	sm11	—3-hydroxy phenyl
sm2	—phenyl	sm12	—2,3,4-trihydroxy phenyl
sm3	—4-nitro phenyl	sm13	—3-methoxy-4-hydroxy phenyl
sm4	—4-bromo phenyl	sm14	—2-methoxy phenyl
sm5	—4-fluoro phenyl	sm15	—4-styryl
sm6	—4-chloro phenyl	sm16	—naphthyl
sm7	—4-methyl phenyl	sm17	—2,4-dinitro phenyl
sm8	—4-methoxy phenyl	sm18	—4-methylsulfonyl phenyl
sm9	—4-hydroxy phenyl	sm19	—4-dimethylamino phenyl
sm10	—3-nitro phenyl	sm20	—4-trifluoromethyl phenyl

Pharmacokinetics and toxicity predictions of designed derivatives

Chemical absorption, distribution, metabolism, excretion, and toxicity (ADMET), play key roles in drug discovery and development. A high-quality drug candidate should not only have sufficient efficacy against the therapeutic target, but also show appropriate ADMET properties at a therapeutic dose. The designed derivatives were screened for its ADME analysis, drug-likeness and toxicity parameters. The Lipinski rule of five and the pharmacokinetic (ADME) characteristics of designed derivatives were investigated using Swiss ADME(29) servers. The toxicity of the compounds has been predicted using ProTox-II, which

is a freely accessible webserver for *in silico* toxicity predictions of new derivatives (http://tox.charite.de/protox_II)(30).

Molecular Docking

All the selected compounds and the native ligand were docked against the crystal structure of the crystal Structure of EGFR T790M mutant in complex with naquotinib using Autodock vina 1.1.2 in PyRx 0.8(1). ChemDraw Ultra 8.0 was used to draw the structures of the compounds and native ligand (mole. File format). All the ligands were subjected for energy minimization by applying Universal Force Field (UFF)(2). The crystal structure of the enzyme with PDB ID 5Y9T was obtained from RCSB Protein Data Bank (PDB) (<https://www.rcsb.org/structure/5Y9T>). Discovery Studio Visualizer (version-19.1.0.18287) was used to refine the enzyme structure, purify it, and get it ready for docking(3). A three-dimensional grid box (size_x=62.5293379415Å; size_y=43.0367205343Å; size_z=43.851824552Å) with an exhaustiveness value of 8 was created for molecular docking(1). BIOVIA Discovery Studio Visualizer was used to locate the protein's active amino acid residues. The approach outlined by Khan et al. was used to perform the entire molecular docking procedure, identify cavity and active amino acid residues(4–10). Fig. 1 shows the revealed cavity of enzyme with the native ligand molecule.

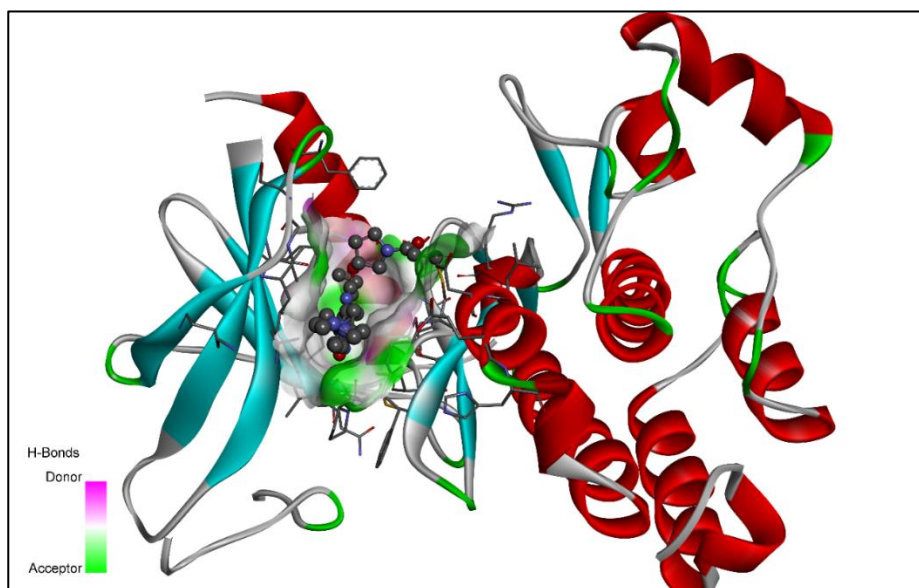


Fig. 1. The 3D ribbon view of the enzyme with native ligand in the cavity

Result and Discussion

Pharmacokinetic characteristics are critical to drug development because they enable scientists to investigate the biological impacts of possible pharmacological candidates(23). This compound's oral bioavailability was evaluated using Lipinski's rule of five and Veber's rules (Table 2). To better understand the pharmacokinetics profiles and drug-likeness properties of the proposed

compounds, the ADME characteristics of all of them were examined (Table 3). The oral acute toxicity have been predicted along with LD₅₀ (mg/kg), toxicity class, hepatotoxicity, carcinogenicity, immunotoxicity, mutagenicity, and cytotoxicity (Table 4). Table 5 depicts the active amino residues, bond length, bond category, bond type, ligand energies, and docking scores. The docking poses of the molecules are exemplified in Table 6.

Table 2
Lipinski rule of 5 and Veber's rule calculated for molecules

Compound Codes	Lipinski rule of five					Veber's rule	
	Log P	Mol. Wt.	HBA	HBD	Violations	Total polar surface area (Å ²)	No. of rotatable bonds
sm1	2.04	224.64	3	0	0	41.9	2
sm2	3.38	300.74	3	0	0	41.9	3
sm3	2.05	346.75	5	1	0	91.56	4
sm4	4.01	379.64	3	0	1	41.9	3
sm5	3.7	318.73	4	0	1	41.9	3
sm6	3.92	335.18	3	0	1	41.9	3
sm7	3.71	314.77	3	0	1	41.9	3
sm8	3.29	330.77	4	0	0	51.13	4
sm9	2.97	316.74	4	1	0	62.13	3
sm10	2.05	346.75	5	1	0	91.56	4
sm11	2.97	316.74	4	1	0	62.13	3
sm12	2.21	348.74	6	3	0	102.59	3
sm13	2.95	346.77	5	1	0	71.36	4
sm14	3.3	330.77	4	0	0	51.13	4
sm15	3.44	328.79	2	0	0	32.78	4
sm16	4.29	350.8	3	0	1	41.9	3
sm17	1.39	392.75	7	2	0	141.22	5
sm18	3.05	378.83	5	0	0	84.42	4
sm19	3.3	343.81	3	0	0	45.14	4
sm20	4.43	368.74	6	0	1	41.9	4

Where: Mol. Wt., molecular weight; HBA, hydrogen bond acceptors; HBD, hydrogen bond donors

Table 3
The pharmacokinetics and drug-likeness properties of developed compounds

Compound codes	Pharmacokinetics	Drug-likeness											
	GI abs.	BBB pen.	P-gp sub.	CYP1 A2 inhibitors	CYP2 C19	CYP2 C9	CYP2 D6	CYP3 A4	Log K_p (skin permeation, cm/s)	Ghose	Egan	Muegge	Bioavailability Score
sm1	High	Yes	No	Yes	No	No	No	No	-6.22	0	0	0	0.55
sm2	High	Yes	No	Yes	Yes	Yes	No	No	-5.6	0	0	0	0.55
sm3	High	No	No	No	No	No	No	No	-6.33	0	0	0	0.55
sm4	High	Yes	No	Yes	Yes	Yes	No	No	-5.59	0	0	0	0.55
sm5	High	Yes	No	No	Yes	Yes	No	No	-5.64	0	0	0	0.55
sm6	High	Yes	No	Yes	Yes	Yes	No	No	-5.36	0	0	0	0.55
sm7	High	Yes	No	No	Yes	Yes	No	No	-5.43	0	0	0	0.55
sm8	High	Yes	No	Yes	Yes	Yes	No	No	-5.8	0	0	0	0.55
sm9	High	Yes	No	Yes	Yes	Yes	No	No	-5.95	0	0	0	0.55
sm10	High	No	No	No	No	No	No	No	-6.33	0	0	0	0.55
sm11	High	Yes	No	Yes	Yes	Yes	No	No	-5.95	0	0	0	0.55
sm12	High	No	No	Yes	No	No	No	No	-6.65	0	0	0	0.55
sm13	High	Yes	No	Yes	Yes	Yes	No	No	-6.15	0	0	0	0.55
sm14	High	Yes	No	Yes	Yes	Yes	No	No	-5.8	0	0	0	0.55
sm15	High	Yes	No	No	Yes	Yes	No	No	-5.37	0	0	0	0.55
sm16	High	Yes	No	Yes	Yes	Yes	No	No	-5.02	0	0	0	0.55
sm17	Low	No	Yes	No	Yes	Yes	No	No	-7.06	0	1	0	0.55
sm18	High	No	No	Yes	Yes	Yes	No	No	-6.62	0	0	0	0.55
sm19	High	Yes	No	No	Yes	Yes	No	No	-5.78	0	0	0	0.55
sm20	High	Yes	No	No	Yes	Yes	No	No	-5.39	0	0	0	0.55

Where: NL, Native ligand; GI abs., gastrointestinal absorption; BBB pen., blood brain barrier penetration; P-gp sub., p-glycoprotein substrate

Table 4
The predicted acute toxicity of molecules

Compo und codes	Parame ters	The predicted acute toxicity of molecules						
	LD ₅₀ (mg/kg)	Toxicity class	Predicti on accurac y (%)	Hepatot oxicity (Probab ility)	Carcino genicity (Probab ility)	Immun otoxicit y (Probab ility)	Mutage nicity (Probab ility)	Cytotox icity (Probab ility)
sm1	3000	5	54.26	I (0.54)	A (0.57)	I (0.97)	I (0.61)	I (0.61)
sm2	1000	4	54.26	A (0.59)	A (0.50)	I (0.96)	I (0.72)	A (0.65)
sm3	3000	5	54.26	A (0.61)	A (0.50)	I (0.73)	I (0.71)	A (0.65)
sm4	700	4	54.26	A (0.60)	I (0.50)	I (0.76)	I (0.71)	A (0.69)
sm5	700	4	54.26	A (0.61)	I (0.50)	I (0.73)	I (0.71)	A (0.68)
sm6	1000	4	54.26	A (0.61)	A (0.50)	I (0.73)	I (0.71)	A (0.65)
sm7	1000	4	54.26	A (0.59)	I (0.51)	I (0.97)	I (0.70)	A (0.63)
sm8	1000	4	54.26	A (0.62)	I (0.53)	I (0.62)	I (0.66)	I (0.70)

sm9	550	4	54.26	A (0.65)	I (0.50)	I (0.90)	I (0.68)	I (0.55)
sm10	3000	5	54.26	A (0.65)	I (0.50)	I (0.90)	I (0.68)	I (0.55)
sm11	1000	4	23	A (0.65)	I (0.50)	I (0.77)	I (0.68)	I (0.55)
sm12	4920	5	23	A (0.63)	I (0.52)	I (0.52)	I (0.68)	I (0.69)
sm13	4920	5	54.26	A (0.64)	I (0.54)	A (0.82)	I (0.67)	I (0.73)
sm14	1000	4	23	A (0.61)	I (0.57)	A (0.53)	I (0.67)	I (0.77)
sm15	300	3	54.26	I (0.52)	I (0.50)	I (0.96)	I (0.68)	I (0.61)
sm16	1000	4	54.26	A (0.58)	I (0.53)	I (0.89)	I (0.76)	A (0.85)
sm17	2201	5	23	A (0.58)	I (0.53)	I (0.89)	I (0.76)	A (0.85)
sm18	4000	5	23	I (0.53)	I (0.59)	I (0.77)	I (0.72)	I (0.68)
sm19	5505	6	54.26	A (0.54)	I (0.62)	I (0.68)	I (0.64)	I (0.60)
sm20	700	4	54.26	A (0.63)	A (0.50)	I (0.89)	I (0.68)	A (0.61)

Where: I, Inactive; A, Active

Table 5
The active amino residues, bond length, bond category, bond type, ligand energies, and docking scores

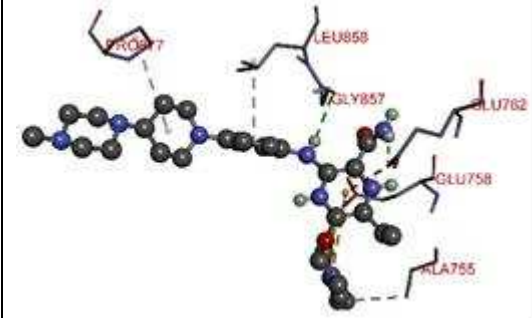
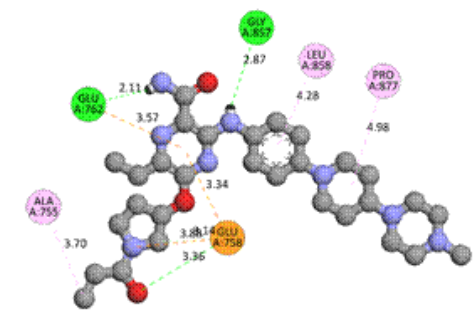
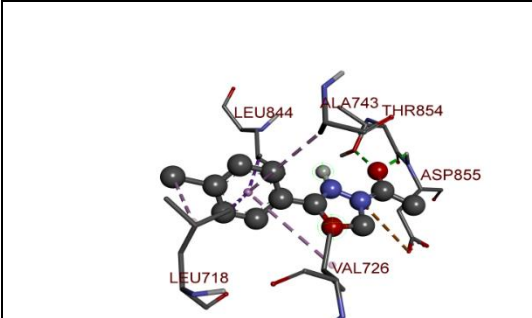
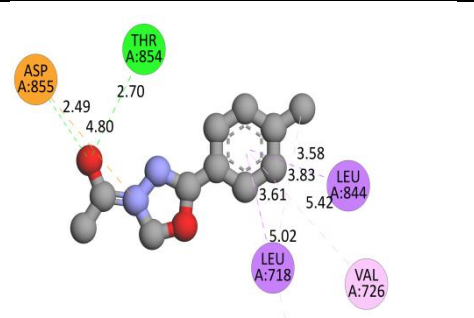
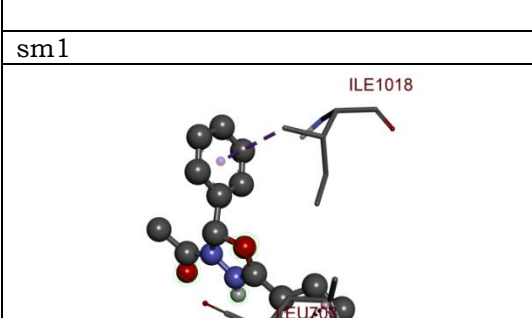
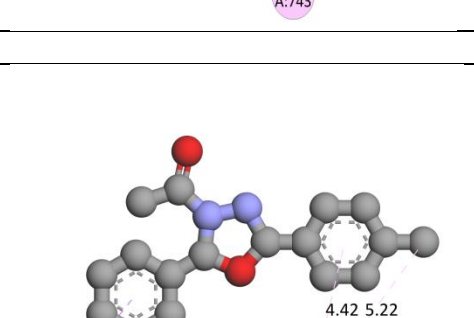
Active amino acids	Bond length	Bond type	Bond category	Ligands energy	Docking score
Native ligand					
GLU758	3.88487	Electrostatic	Attractive Charge	568.59	-8.3
GLY857	2.87344	Hydrogen Bond	Conventional Hydrogen Bond		
GLU762	2.10926		Carbon Hydrogen Bond		
GLU758	3.35859				
GLU758	3.13642	Electrostatic	Pi-Anion		
GLU758	3.33922				
GLU762	3.56702				
ALA755	3.69661	Hydrophobic	Alkyl		
PRO877	4.97918		Pi-Alkyl		
LEU858	4.28035				
sm1					
ASP855	4.80189	Electrostatic	Attractive Charge	304.76	-6
THR854	2.70059	Hydrogen Bond	Conventional Hydrogen Bond		
ASP855	2.49241		Hydrophobic		
LEU718	3.6134	Alkyl			
LEU844	3.58116	Pi-Alkyl			
LEU718	3.82636				
VAL726	5.42251				
ALA743	5.01938				
sm2					
ILE1018	3.56188	Hydrophobic	Pi-Sigma	461.68	-8.2
LEU703	5.22421		Alkyl		
LEU703	4.42024		Pi-Alkyl		
sm3					
THR854	3.16086	Hydrogen Bond	Conventional Hydrogen Bond	449.4	-8.3
GLU762	2.44501				

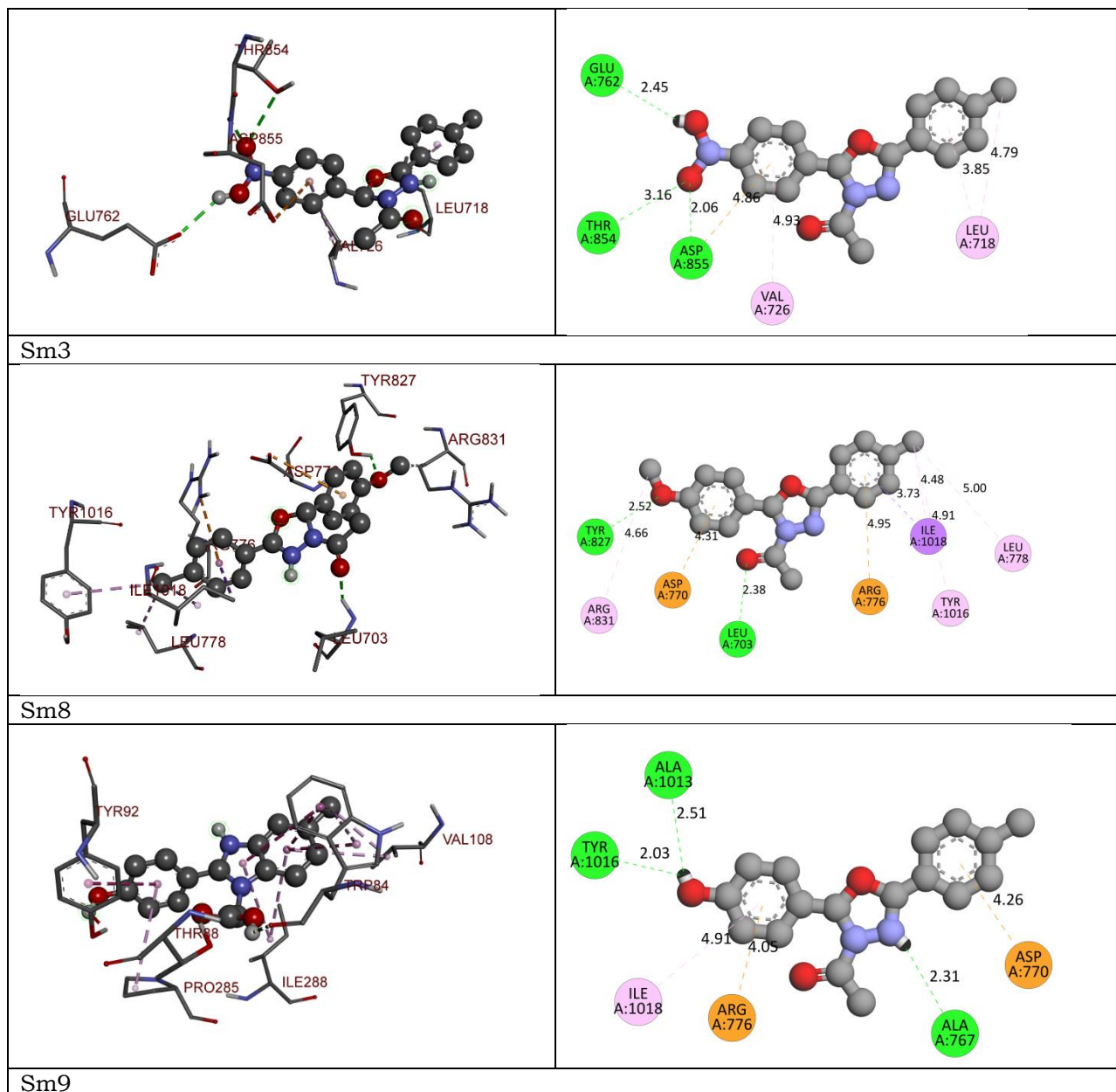
ASP855	2.06482				
ASP855	4.85569	Electrostatic	Pi-Anion		
LEU718	4.78982	Hydrophobic	Alkyl		
VAL726	4.93425		Pi-Alkyl		
LEU718	3.8475				
sm4					
LEU718	3.92364	Hydrophobic	Pi-Sigma	466.2	-8.2
LEU718	4.53559		Alkyl		
VAL726	5.49873		Pi-Alkyl		
sm5					
			Conventional Hydrogen Bond;Halogen (Fluorine)	346.51	-8.1
LYS745	2.01835	Hydrogen Bond;Halogen	Halogen (Fluorine)		
GLU762	3.67342	Halogen	Halogen (Fluorine)		
ASP855	4.58384	Electrostatic	Pi-Anion		
LEU718	3.98999	Hydrophobic	Pi-Sigma		
LEU844	3.54568		Alkyl		
LEU718	4.37964		Pi-Alkyl		
VAL726	5.34235				
MET790	5.33612				
sm6					
LEU718:O	2.33685	Hydrogen Bond	Conventional Hydrogen Bond	359.49	-8.0
ASP855	4.48375	Electrostatic	Pi-Anion		
MET790	4.83339	Hydrophobic	Alkyl		
VAL726	4.50617		Pi-Alkyl		
VAL726	5.25874				
LEU718	3.92772				
sm7					
ASP855	4.43382	Electrostatic	Pi-Anion	322.46	-8.0
LEU718	3.9588	Hydrophobic	Pi-Sigma		
LEU844	3.5256		Alkyl		
LYS745	5.21002				
MET790	4.76992				
LEU718	4.30575				
MET790	5.39316		Pi-Alkyl		
LEU844	5.47259				
sm8					
LEU703	2.38234	Hydrogen Bond	Conventional Hydrogen Bond	494.79	-8.7
TYR827	2.52106				
ARG776	4.94776	Electrostatic	Pi-Cation		
ASP770	4.30886		Pi-Anion		
ILE1018	3.72929	Hydrophobic	Pi-Sigma		
ARG831	4.66377		Alkyl		
LEU778	5.00032				
ILE1018	4.48071				
TYR1016	4.91462				

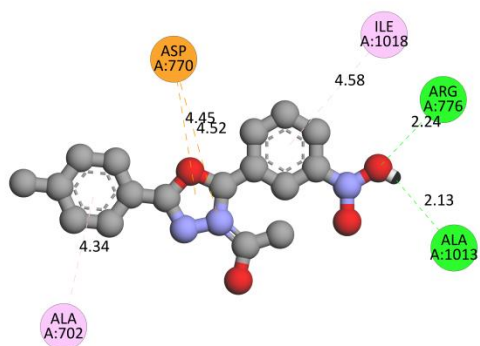
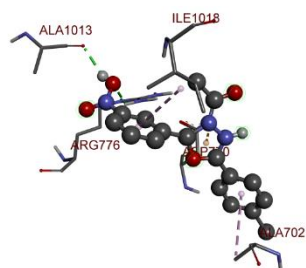
sm9					
ALA767	2.31174	Hydrogen Bond	Conventional Hydrogen Bond	457.81	-8.5
ALA1013	2.51271				
TYR1016	2.03423				
ARG776	4.04585	Electrostatic	Pi-Cation		
ASP770	4.25988		Pi-Anion		
ARG776	5.36441	Hydrophobic	Pi-Alkyl		
ILE1018	4.91446				
sm10					
ASP770	4.51903	Electrostatic	Attractive Charge	774.68	-8.7
ALA1013	2.12736	Hydrogen Bond	Conventional Hydrogen Bond		
ARG776	2.23577		Conventional Hydrogen Bond		
A:ASP770	4.45104	Electrostatic	Pi-Anion		
ILE1018	4.57745	Hydrophobic	Pi-Alkyl		
ALA702	4.34458				
sm11					
ASP855	4.6377	Electrostatic	Pi-Anion	341.44	-8.1
LEU844	3.52938	Hydrophobic	Pi-Sigma		
LEU718	4.47331		Alkyl		
VAL726	5.16417		Pi-Alkyl		
MET790	5.37716		Pi-Alkyl		
LEU718	3.85611		Pi-Alkyl		
sm12					
GLN701	3.19535	Hydrogen Bond	Conventional Hydrogen Bond	312.33	-8.6
SER768	1.86175				
TYR827	2.39179				
TYR827	2.87448				
ASP770	4.19161	Electrostatic	Pi-Anion		
ILE1018	3.91424	Hydrophobic	Pi-Sigma		
LEU778	4.49671		Alkyl		
ILE1018	4.44808				
sm13					
LEU703	2.44512	Hydrogen Bond	Conventional Hydrogen Bond	338.83	-8.8
ARG776:	4.93935	Electrostatic	Pi-Cation		
ILE1018	3.70366	Hydrophobic	Pi-Sigma		
LEU778	5.17816		Alkyl		
ILE1018	4.38419				
TYR1016	4.85315		Pi-Alkyl		
sm14					
ARG841	3.51246	Hydrogen Bond	Carbon Hydrogen Bond	334.32	-8.2
ASN842	3.59968		Carbon Bond		
LEU718	3.91693	Hydrophobic	Pi-Sigma		
LEU718	4.49092		Alkyl		
VAL726	5.26015		Pi-Alkyl		
sm15					
ALA767	3.31618	Hydrogen Bond	Carbon Hydrogen Bond	314.49	-8.2
ASP770	3.61071		Carbon Bond		

LEU1017	3.68846	Hydrophobic	Pi-Sigma		
LEU778	4.11015		Alkyl		
ILE1018	4.65007		Pi-Alkyl		
ILE1018	4.87111				
TRP731	5.32319				
TYR1016	5.45835				
sm16					
ASP770	5.12621	Electrostatic	Attractive Charge	450.85	-8.4
:LEU703	3.00373	Hydrogen Bond	Pi-Donor Hydrogen Bond		
ILE1018	3.435	Hydrophobic	Pi-Sigma		
ILE1018	3.64982		Pi-Alkyl		
LEU703	5.2363				
LEU703	5.15416				
sm17					
LEU777	2.25265	Hydrogen Bond	Conventional Hydrogen Bond	445.15	-8.1
LEU778	2.24662				
LEU703	3.89849	Hydrophobic	Pi-Sigma		
LEU703	5.30319		Alkyl		
ILE1018	4.52615		Pi-Alkyl		
sm18					
ASP770	3.66561	Electrostatic	Attractive Charge	450.16	-8.1
ASN700	2.0857	Hydrogen Bond	Conventional Hydrogen Bond		
ASN700	2.73068				
GLN701	2.10706				
ASP770	4.17503	Electrostatic	Pi-Anion		
ILE1018	3.9243	Hydrophobic	Pi-Sigma		
LEU778	4.32332		Alkyl		
ILE1018	4.56006				
ALA702	4.58581		Pi-Alkyl		
sm19					
ASP855	2.99904	Hydrogen Bond	Conventional Hydrogen Bond	337.45	-8.3
ASP855	3.47705	Electrostatic	Pi-Anion		
LEU718	3.39223	Hydrophobic	Pi-Sigma		
LEU844	3.78158		Alkyl		
LEU718	3.8247				
LEU792	5.22053		Pi-Alkyl		
ALA743	5.09194				
PHE723	4.35843				

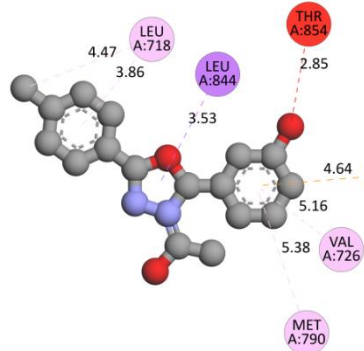
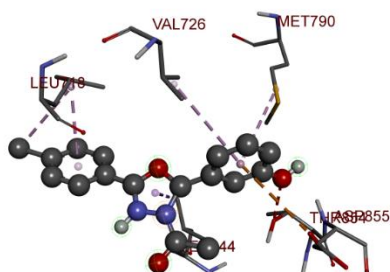
Table 6
The 3D- and 2D-docking poses of the molecules

3D-docking poses	2D-docking poses
	
Native ligand	
	
sm1	
	
sm2	

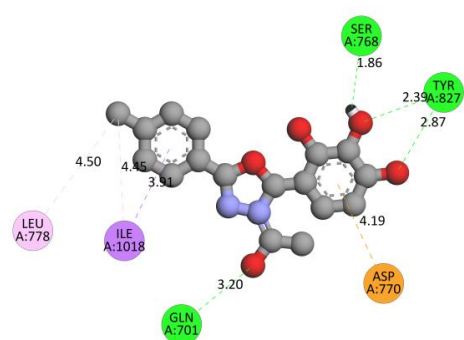
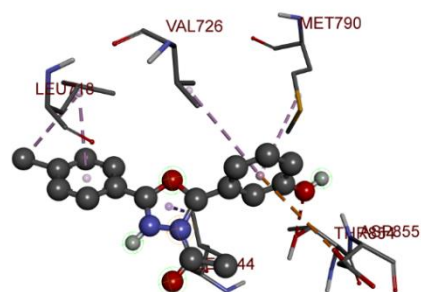




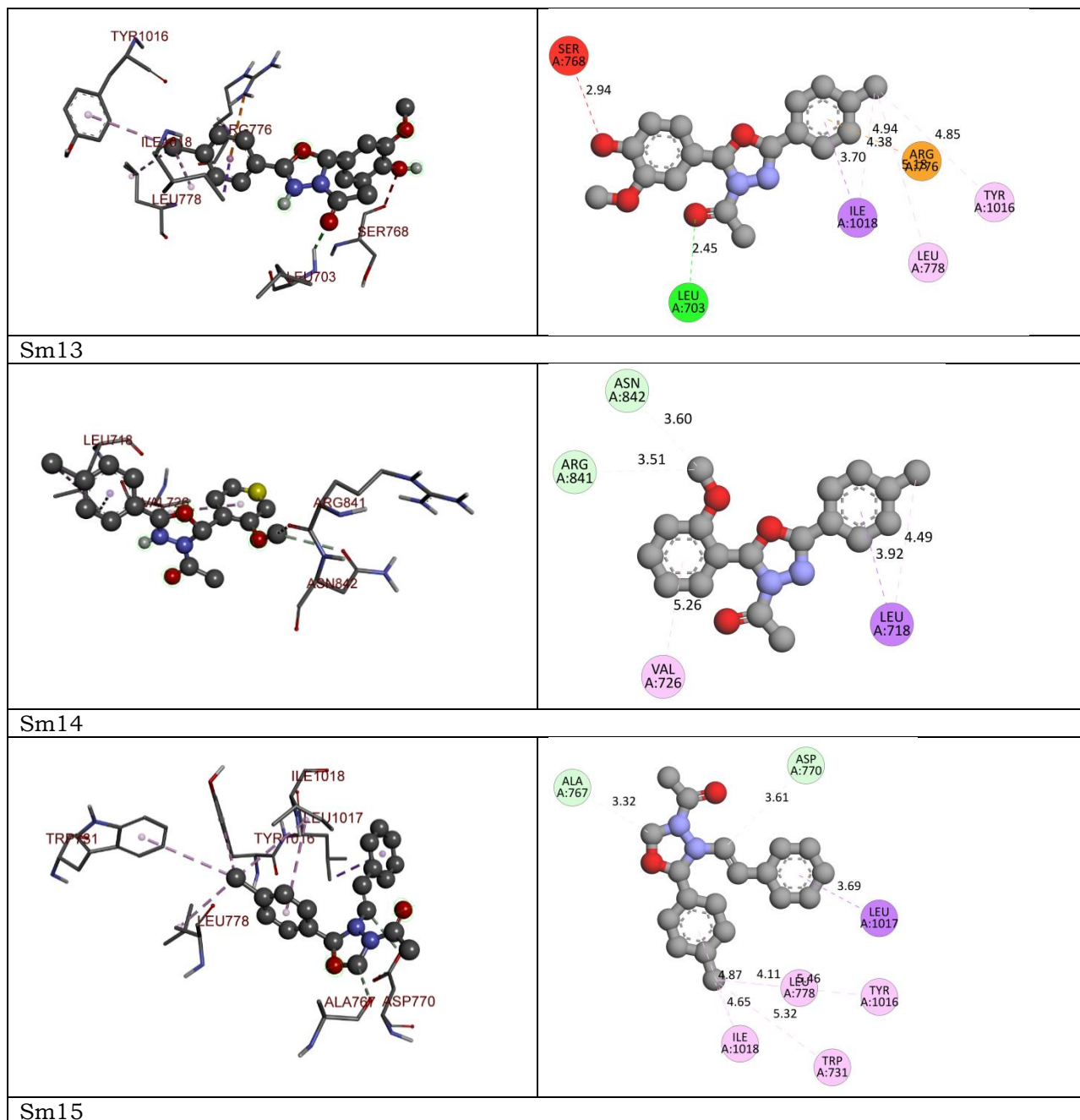
Sm10

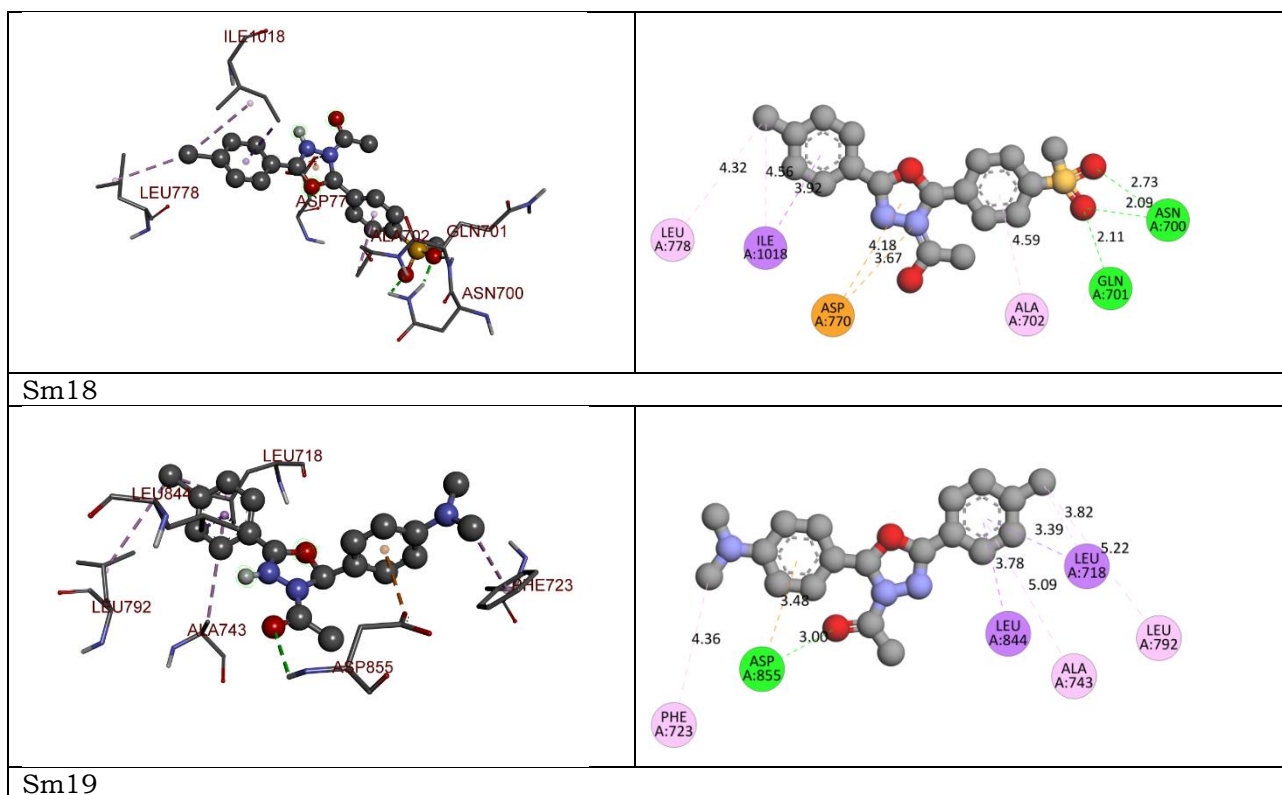


Sm11



Sm12





In present study we have designed and developed some 1-(5-(4-chlorophenyl)-1, 3, 4-oxadiazol-3(2*H*)-yl)ethanone derivatives as potential EGFR inhibitors. In accordance with Lipinski's and Veber's rule (Table 2). The log P values of all the molecules were between the ranges 1.39 to 4.43 which indicates optimum lipophilicity. Lipophilicity is a significant feature of the molecule that affects how it works in the body(27). It is determined by the compound's Log P value, which measures the drug's permeability in the body to reach the target tissue(31,32). The molecular weight of all the molecules was around 500 Da which indicates active better transport of the molecules through biological membrane. Fortunately, the Lipinski rule of 5 had not been compromised by the compounds(23,24). All the compounds except sm4, sm5, sm6, sm7, sm16, sm20 violated the Lipinski rule of 5 .The total polar surface area (TPSA) and the number of rotatable bonds have been found to better discriminate between compounds that are orally active or not. According to Veber's rule, TPSA should be ≤ 140 and number of rotatable bonds should be ≤ 10 . It was observed that, compound sm17 violated the Veber's rule, as it has TPSA 141\AA^2 .

In order to further optimize the compounds, pharmacokinetics and drug-likeness properties were calculated for each one. All the compounds showed no penetration to the blood-brain barrier (BBB). The log *K_p* (skin penetration, cm/s) and bioavailability values of all the compounds were within acceptable limits. (Table 3).The GI absorption of all the compounds was found to be high except for sm17. In acute toxicity predictions, class-III i.e. toxic if swallowed ($50 < LD_{50} \leq 300$), toxicity class-IV which means harmful if swallowed ($300 < LD_{50} \leq 2000$), class-V

which indicate may be harmful if swallowed ($2000 < LD_{50} \leq 5000$)(30). From this virtual screening, it was concluded that all the compounds fall in class IV, V & VI of toxicity, which means they possess drug-like properties and hence were subjected to molecular docking studies. Out of 20 screened molecules through ADMET analysis, compound sm17 displayed low absorption and toxicity class-II therefore eliminated from further screening. The binding affinities of the derivatives have been compared with the binding mode of native ligand present in the crystal structure of EGFR enzyme (PDB ID: 5Y9T).

Native ligand (naquotinib) displayed -8.3 kcal/mol binding affinity with EGFR and formed three conventional and one carbon-hydrogen bond with Gly857, Glu762, and Glu758. It has developed electrostatic (Pi-anion, attractive charge) and hydrophobic bonds (alkyl and Pi-alkyl) with Glu758, Glu762, Ala755, Pro877, and Leu858. All the designed molecules displayed most potent interactions than the native ligand. Many derivatives exhibited more than two hydrogen bonds with the target. The compounds which have formed three or more hydrogen bonds have been selected for the synthesis and biological activity. The formation of hydrogen bonds with target can effectively modulate the activity of enzyme and exhibit potent pharmacological response. There are many compounds which exhibited more binding affinity but did not formed more than three hydrogen bonds, in that case some more derivatives selected for the synthesis. The compound sm1, sm2, sm3, sm8, sm9, sm10, sm11, sm12, sm13, sm14, sm15, sm18, and sm19 has been selected as most potent molecules from virtual screening.

Compound sm1 exhibited -6 kcal/mol binding affinity and formed two conventional hydrogen bonds with Thr854 and Asp855. It displayed many hydrophobic interactions (pi-sigma, alkyl and Pi-alkyl) with Leu718, Leu844, Val726 & Ala743. Compound sm2 showed -7.6 kcal/mol binding affinity and it also displayed many hydrophobic interactions (pi-sigma, alkyl and Pi-alkyl) with Ile1018 & Leu703. Compound sm3 displayed -7.7 kcal/mol binding affinity and it also formed three conventional hydrogen bonds with Thr854, Glu762 and Asp855. It also showed pi-anion type of electrostatic interactions with Asp855. It displayed many hydrophobic interactions (alkyl and Pi-alkyl) with Leu718 & Val726. Compound sm8 exhibited -8.3 kcal/mol binding affinity and it formed two conventional hydrogen bonds with Leu703 and Tyr827. It has developed one Pi-donor hydrogen bond with Trp22 and one electrostatic (Pi-anion) bond with Asp770. It displayed many hydrophobic interactions (alkyl and Pi-alkyl) with Arg831, Leu778, Ile 1018 & Tyr1016.

Compound sm9 showed -7.8 kcal/mol binding affinity and it formed three conventional hydrogen bonds with Ala767, Ala1013 and Tyr1016. It has developed two electrostatic (Pi-cation, Pi-anion) bonds with Asp776 & Asp770. It displayed hydrophobic interactions (Pi-alkyl) with Arg776 & Ile1018. Compound sm10 displayed -7.8 kcal/mol binding affinity and it formed two conventional hydrogen bonds with Arg776 & Ala1013. It has developed one electrostatic (Pi-anion) bond with Asp770. It displayed hydrophobic interactions (Pi-alkyl) with Arg776 & Ile1018. Compound sm11 exhibited -7.1 kcal/mol binding affinity and it has developed one electrostatic (Pi-anion) bond with Asp855. It displayed hydrophobic interactions (Pi-sigma, alkyl, Pi-alkyl) with leu718, Val726 & Met790. Compound sm12 exhibited -7.6 kcal/mol binding affinity and it has developed

one electrostatic (Pi-anion) bond with Asp770. It displayed hydrophobic interactions (Pi-sigma, alkyl,) with Ile1018 & leu778.

Compound sm13 exhibited -7.8 kcal/mol binding affinity and it has developed one electrostatic (Pi-anion) bond with Asp855. It displayed hydrophobic interactions (Pi-sigma, alkyl, Pi-alkyl) with leu778, Ile1018 & Tyr1016. Compound sm14 exhibited -7.5 kcal/mol binding affinity and formed two hydrogen bonds with Arg841 & Asn842. It displayed hydrophobic interactions (Pi-sigma, alkyl, Pi-alkyl) with leu718 & Val726. Compound sm15 exhibited -7.2 kcal/mol binding affinity and formed two hydrogen bonds with Ala767 & Asp770. It displayed hydrophobic interactions (Pi-sigma, alkyl, Pi-alkyl) with leu1017, Leu778, Ile1018, Trp731 & Tyr1016. Compound sm18 displayed -7.1 kcal/mol binding affinity and it also formed three hydrogen bonds with Asn700 & Gln701. It has developed hydrophobic interactions (Pi-sigma, alkyl, Pi-alkyl) with Leu778, Ile778 & Ile1018. Compound sm19 exhibited -7.3 kcal/mol binding affinity and it has developed one electrostatic (Pi-anion) bond with Asp855. It displayed hydrophobic interactions (Pi-sigma, alkyl, Pi-alkyl) with leu718, Leu844, Leu792, Ala743 & Phe723. From above screening it was observed that native ligand formed three conventional hydrogen bonds therefore, the molecules which formed two or more conventional hydrogen bonds with enzyme are considered as most potent and selected for wet lab synthesis followed by biological evaluation. Molecules Sm3, Sm8, Sm9, Sm10, Sm12, and Sm2 had formed either three or two conventional hydrogen bonds with EGFR enzyme and hence selected for synthesis.

Conclusion

A lot of *in silico* models are developed for prediction of chemical ADMET properties. However, it is still not easy to evaluate the drug-likeness of compounds in terms of so many ADMET properties. In present study, we have designed some 1-(5-(4-chlorophenyl)-1, 3, 4-oxadiazol-3(2*H*)-yl) ethanone derivatives to be developed as potential EGFR inhibitors for the treatment of cancer. The designed derivatives were screened through Lipinski rule, Veber's rule, ADMET analysis, drug-likeness properties and molecular docking. We concluded that all the compounds sm1, sm2, sm3, sm8, sm9, sm10, sm11, sm12, sm13, sm14, sm15, sm18, and sm19 were found to possess drug-likeness properties and therefore were subjected for molecular docking studies. From molecular docking studies it was observed that Molecules Sm3, Sm8, Sm9, Sm10, Sm12, and Sm2 had formed either three or two conventional hydrogen bonds with EGFR enzyme and hence selected for synthesis which can be developed further to get more promising molecules for the treatment of cancer.

Acknowledgments

The authors are thankful to Dr. P. Y. Pawar, Principal of Dr. Vitthalrao Vikhe patil foundation's, College of Pharmacy, Vilad Ghat, Ahmednagar for providing the necessary facilities to carry out the research work. Furthermore, authors are also thankful to the people who directly and indirectly help me to carry to this research work.

References

1. Chan DLH, Segelov E, Wong RSH, Smith A, Herbertson RA, Li BT, et al. Epidermal growth factor receptor (EGFR) inhibitors for metastatic colorectal cancer. Vol. 2017, Cochrane Database of Systematic Reviews. 2017.
2. Grünwald V, Hidalgo M. Developing inhibitors of the epidermal growth factor receptor for cancer treatment. Vol. 95, Journal of the National Cancer Institute. 2003. p. 851–67.
3. Song Z, Ge Y, Wang C, Huang S, Shu X, Liu K, et al. Challenges and perspectives on the development of small-molecule EGFR inhibitors against T790M-mediated resistance in non-small-cell lung cancer: Miniperspective. Vol. 59, Journal of Medicinal Chemistry. 2016. p. 6580–94.
4. Harari PM. Epidermal growth factor receptor inhibition strategies in oncology. Vol. 11, Endocrine-Related Cancer. 2004. p. 689–708.
5. Woodburn JR. The epidermal growth factor receptor and its inhibition in cancer therapy. In: Pharmacology and Therapeutics. 1999. p. 241–50.
6. Chen L, Fu W, Zheng L, Liu Z, Liang G. Recent Progress of Small-Molecule Epidermal Growth Factor Receptor (EGFR) Inhibitors against C797S Resistance in Non-Small-Cell Lung Cancer. Vol. 61, Journal of Medicinal Chemistry. 2018. p. 4290–300.
7. Attili I, Karachaliou N, Conte PF, Bonanno L, Rosell R. Therapeutic approaches for T790M mutation positive non-small-cell lung cancer. Expert Rev Anticancer Ther. 2018;18(10):1021–30.
8. Ai X, Guo X, Wang J, Stancu AL, Joslin PMN, Zhang D, et al. Targeted therapies for advanced non-small cell lung cancer. Oncotarget. 2018;9(101):37589–607.
9. Bryce AH, Rao R, Sarkaria J, Reid JM, Qi Y, Qin R, et al. Phase i study of temsirolimus in combination with EKB-569 in patients with advanced solid tumors. Invest New Drugs. 2012;30(5):1934–41.
10. Grünwald V, Hidalgo M. Developing inhibitors of the epidermal growth factor receptor for cancer treatment. J Natl Cancer Inst. 2003;95(12):851–67.
11. Roskoski R. Cyclin-dependent protein kinase inhibitors including palbociclib as anticancer drugs. Pharmacol Res [Internet]. 2016;107:249–75. Available from: <http://dx.doi.org/10.1016/j.phrs.2016.03.012>
12. Gokhale N, Dalimba U, Kumsi M. Facile synthesis of indole-pyrimidine hybrids and evaluation of their anticancer and antimicrobial activity. J Saudi Chem Soc [Internet]. 2017;21(7):761–75. Available from: <http://dx.doi.org/10.1016/j.jscs.2015.09.003>
13. Saavedra LM, Ruiz D, Romanelli GP, Duchowicz PR. Quantitative Structure-Antifungal Activity Relationships for cinnamate derivatives. Ecotoxicol Environ Saf [Internet]. 2015;122:521–7. Available from: <http://dx.doi.org/10.1016/j.ecoenv.2015.09.024>
14. Lv PC, Li DD, Li QS, Lu X, Xiao ZP, Zhu HL. Synthesis, molecular docking and evaluation of thiazolyl-pyrazoline derivatives as EGFR TK inhibitors and potential anticancer agents. Bioorganic Med Chem Lett. 2011;21(18):5374–7.
15. Bhadoriya KS, Kumawat NK, Bhavthankar S V., Avchar MH, Dhumal DM, Patil SD, et al. Exploring 2D and 3D QSARs of benzimidazole derivatives as transient receptor potential melastatin 8 (TRPM8) antagonists using MLR and kNN-MFA methodology. J Saudi Chem Soc [Internet]. 2016;20:S256–70. Available from: <http://dx.doi.org/10.1016/j.jscs.2012.11.001>

16. Galayev O, Garazd Y, Garazd M, Lesyk R. Synthesis and anticancer activity of 6-heteroaryl coumarins. *Eur J Med Chem* [Internet]. 2015;105:171–81. Available from: <http://dx.doi.org/10.1016/j.ejmech.2015.10.021>
17. Akhtar W, Khan MF, Verma G, Shaquiquzzaman M, Rizvi MA, Mehdi SH, et al. Therapeutic evolution of benzimidazole derivatives in the last quinquennial period. *Eur J Med Chem* [Internet]. 2017;126:705–53. Available from: <http://dx.doi.org/10.1016/j.ejmech.2016.12.010>
18. Mohana Roopan S, Sompalle R. Synthetic chemistry of pyrimidines and fused pyrimidines: A review. *Synth Commun*. 2016;46(8):645–72.
19. Gil A, Pabón A, Galiano S, Burguete A, Pérez-Silanes S, Deharo E, et al. Synthesis, biological evaluation and structure-activity relationships of new quinoxaline derivatives as anti-Plasmodium falciparum agents. *Molecules*. 2014;19(2):2166–80.
20. Ghorab MM, Ragab FA, Heiba HI, El-Gazzar MG, Zahran SS. Synthesis, anticancer and radiosensitizing evaluation of some novel sulfonamide derivatives. *Eur J Med Chem* [Internet]. 2015;92:682–92. Available from: <http://dx.doi.org/10.1016/j.ejmech.2015.01.036>
21. Khan SL, Siddiqui FA, Shaikh MS, Nema N V., Shaikh AA. Discovery of potential inhibitors of the receptor-binding domain (RBD) of pandemic disease-causing SARS-CoV-2 Spike Glycoprotein from Triphala through molecular docking. *Curr Chinese Chem* [Internet]. 2021;01. Available from: <https://www.eurekaselect.com/192390/article>
22. Siddiqui FA, Khan SL, Marathe RP, Nema N V. Design, Synthesis, and In Silico Studies of Novel N-(2-Aminophenyl)-2,3-Diphenylquinoxaline-6-Sulfonamide Derivatives Targeting Receptor-Binding Domain (RBD) of SARS-CoV-2 Spike Glycoprotein and their Evaluation as Antimicrobial and Antimalarial Agents. *Lett Drug Des Discov* [Internet]. 2021;18(9):915–31. Available from: <https://doi.org/10.2174/1570180818666210427095203>
23. Khan A, Unnisa A, Soheli M, Date M, Panpaliya N, Saboo SG, et al. Investigation of phytoconstituents of *Enicostemma littorale* as potential glucokinase activators through molecular docking for the treatment of type 2 diabetes mellitus. *Silico Pharmacol* [Internet]. 2022;10(1). Available from: <https://doi.org/10.1007/s40203-021-00116-8>
24. Shntaif AH, Khan S, Tapadiya G, Chettupalli A, Saboo S, Shaikh MS, et al. Rational drug design, synthesis, and biological evaluation of novel N-(2-arylaminophenyl)-2,3-diphenylquinoxaline-6-sulfonamides as potential antimalarial, antifungal, and antibacterial agents. *Digit Chinese Med* [Internet]. 2021;4(4):290–304. Available from: <https://www.sciencedirect.com/science/article/pii/S2589377721000483>
25. Khan, Sharuk L; Siddiqui FA. Beta-Sitosterol: As Immunostimulant, Antioxidant and Inhibitor of SARS-CoV-2 Spike Glycoprotein. *Arch Pharmacol Ther*. 2020;2(1).
26. Chaudhari RN, Khan SL, Chaudhary RS, Jain SP, Siddiqui FA. B-Sitosterol: Isolation from *Muntingia Calabura* Linn Bark Extract, Structural Elucidation And Molecular Docking Studies As Potential Inhibitor of SARS-CoV-2 Mpro (COVID-19). *Asian J Pharm Clin Res*. 2020;13(5):204–9.
27. Khan S, Kale M, Siddiqui F, Nema N. Novel pyrimidine-benzimidazole hybrids with antibacterial and antifungal properties and potential inhibition of SARS-CoV-2 main protease and spike glycoprotein. *Digit Chinese Med*. 2021;4(2):102–19.

28. Khan SL, Sonwane GM, Siddiqui FA, Jain SP, Kale MA, Borkar VS. Discovery of Naturally Occurring Flavonoids as Human Cytochrome P450 (CYP3A4) Inhibitors with the Aid of Computational Chemistry. *Indo Glob J Pharm Sci.* 2020;10(04):58–69.
29. Daina A, Michielin O, Zoete V. SwissADME: A free web tool to evaluate pharmacokinetics, drug-likeness and medicinal chemistry friendliness of small molecules. *Sci Rep.* 2017;7.
30. Banerjee P, Eckert AO, Schrey AK, Preissner R. ProTox-II: A webserver for the prediction of toxicity of chemicals. *Nucleic Acids Res.* 2018;46(W1):W257–63.
31. Krzywinski M, Altman N. Points of significance: Significance, P values and t-tests. *Nat Methods.* 2013;10(11):1041–2.
32. Lipinski CA, Lombardo F, Dominy BW, Feeney PJ. Experimental and computational approaches to estimate solubility and permeability in drug discovery and development settings. Vol. 64, *Advanced Drug Delivery Reviews.* 2012. p. 4–17.